Quantum Critical Dynamics Induced by Topological Zero Modes

Ilia Komissarov,[1, *] Tobias Holder,[2, †] and Raquel Queiroz[1, 3, ‡]

[1]*Department of Physics, Columbia University, New York, NY 10027, USA*
[2]*School of Physics and Astronomy, Tel Aviv University, Tel Aviv, Israel*
[3]*Center for Computational Quantum Physics, Flatiron Institute, New York, New York 10010, USA*
(Dated: February 19, 2025)

We investigate the low-frequency ac transport in the Su-Schrieffer-Heeger (SSH) chain with chiral disorder near the topological delocalization transition. Our key finding is that the formation of hybridized pairs of topological domain wall zero modes leads to the anomalous logarithmic scaling of the ac conductivity $\sigma(\omega) \sim \log \omega$ at criticality, and $\sigma(\omega) \sim \omega^{2\delta} \log^2 \omega$ away from it. Using the combination of real-space renormalization group analysis and qualitative hybridization arguments, we demonstrate that the form of the scaling of ac conductivity at criticality stems directly from the stretched-exponential ($\psi(x) \sim e^{-s\sqrt{x}}$) spatial decay of zero-mode wavefunctions at the critical point.

Introduction.— Transport phenomena in disordered topological insulators exhibit behavior strikingly different from their trivial counterparts. For example, some subset of electronic states may become delocalized even in low-dimensional systems — a prominent example being the quantum Hall plateau transition [1–4] which, despite many years of research, is still poorly understood [5]. A simpler and more tractable model that displays similar behavior is the Su-Schrieffer-Heeger (SSH) chain [6] with chiral disorder, i.e. with disorder in hopping elements only. In this model, exactly one mode at zero energy becomes delocalized when the geometric averages of even and odd hopping elements are equal [7, 8].

Many aspects of quantum critical behavior in this model and the ones in the same universality class were extensively studied [9–14], and observed experimentally in disordered atomic wires [15]. The renormalization group flow equations were solved analytically [16, 17] providing access to exact results such as the low-energy density of states and critical exponents. For the continuous $1D$ fermion model with random mass, characterized by the same fixed point, it has been shown that at criticality, charge carriers exhibit a logarithmically slow spreading of probability density [18, 19]. In this work, we obtain a remarkable manifestation of this behavior in the form of the logarithmic scaling of low-frequency ac conductivity

$$\sigma_{\text{crit}}(\omega) \sim \log(\Omega/\omega), \tag{1}$$

where Ω is a high-energy reference scale. This form of ac conductivity is highly atypical: as the frequency ω is decreased, we would expect the number of states participating in transport to decrease polynomially due to Pauli blocking. This would lead to insulating behavior as it occurs in the chain with purely on-site disorder (Anderson model) where $\sigma_{\text{MB}}(\omega) \sim \omega^2 \log^2 \omega$, according to the Mott-Berezinskiy law [20–22]. Instead, in the case of the SSH chain with chiral disorder and at criticality, the divergence of the density of the in-gap states induced by the fluctuations in the winding number introduced by impurities (Dyson singularity [1, 23]) compensates for the
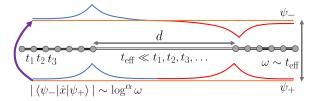

Figure 1. Hopping disorder in the SSH chain creates isolated rare regions characterized by extremely small effective tunneling probability t_{eff}. Two zero modes appearing on both sides of the link t_{eff} hybridize away from zero energy with energy splitting $\omega \sim t_{\text{eff}} \sim e^{-\sqrt[\alpha]{d/\xi}}$, where ξ encodes the typical size of individual zero modes and both $\alpha = 1$ and $\alpha = 2$ are possible in this model. The transition amplitude between these states in ac electric field is $|\langle \psi_- |\hat{x}| \psi_+ \rangle| \sim d \sim \log^\alpha \omega$, implying an insulator for $\alpha = 1$ with ac conductivity following a modified Mott-Berezinskiy law (2), and, for $\alpha = 2$, a glassy metal characterized by activated dynamical scaling (1).

Pauli blocking effects, and the dc conductivity diverges. This divergence is, however, only logarithmic in frequency, which indicates the tunneling regime of electronic propagation with the vanishing Drude weight, in contrast to the "free acceleration" $\sigma(\omega) \sim \omega^{-1}$ form [24] typical in conventional metals. Therefore, the appearance of (1) highlights a remarkable situation in which the topology almost exactly counteracts the localizing effects of disorder giving rise to logarithmically slow "glassy" behavior of the ac conductivity. We note that using chiral disorder is crucial for this behavior as on-site impurities would lower the symmetry to the topologically trivial Anderson model without a divergent density of states.

We also argue that away from the critical point, the form of the ac conductivity in the SSH chain with chiral disorder assumes the form

$$\sigma(\omega) \sim \omega^{2\delta} \log^2 \omega, \tag{2}$$

with $\delta > 0$ parameterizing the distance to the critical point [25]. Notably, $2\delta = z^{-1}$, where z is the dynamical critical exponent. Thus, if δ approaches zero, z diverges, giving way to the activated behavior of Eq. (1). In $\delta > 0$ case,

the dc conductivity vanishes since the divergence in the density of zero modes is milder than in the critical case and insufficient to compensate for the reduction of low energy excitations with energy ω.

The expressions Eqs. (1), (2) constitute the main result of this work, and we establish their validity both analytically and numerically. Our analytical approach follows the framework introduced by Mott [20], who proposed that special rare resonating states dominate the ac conductivity in the Anderson model. We demonstrate that in the SSH chain with chiral disorder, we can similarly identify a relevant subset of states between which the matrix element of the dipole operator diverges at small ω. We show that the role of such states is played by bonding (ψ_+) and anti-bonding (ψ_-) orbitals formed by hybridizing pairs of topological zero modes (see Fig. 1). The dipole transition amplitude between $|\psi_+\rangle$ and $|\psi_-\rangle$ at low ω behaves as $\log \omega$ away from criticality and $\log^2 \omega$ exactly at the critical point due to the exponential and the stretched-exponential decay of the wavefunctions of zero modes [13]. The scaling laws for the transition amplitude between $|\psi_\pm\rangle$ together with the behavior of the density of states are sufficient to find the low-frequency ac conductivity Eqs. (1), (2).

We note that dynamical properties similar to Eq. (1) and Eq. (2) were obtained previously near superconductor-metal transitions [26], many-body localized phases [27], and in $1D$ Ising magnets [28]. However, the approach we adopt in this work significantly differs from the ones in the existing literature. Our objective is to highlight the importance of topological zero modes and their hybridized pairs in the low-frequency dynamical behavior of disordered critical topological systems. Using this approach, we are also able to obtain the transport properties at relatively high energy scales, which are inaccessible for the renormalization group techniques usually employed to study this critical point. In particular, a smooth crossover between the regimes Eq. (1), Eq. (2) naturally follows.

In the following, we study the low-frequency dynamics of the SSH chain with bond dilution as an intuitive example elucidating the role of the resonances of zero modes in transport. The case of continuous bond disorder distributions follows from similar considerations. Finally, we present analytical and numerical evidence that at criticality the transition amplitude between the Mott resonances scales as $\log^2 \omega$, giving rise to the activated scaling of low-frequency ac conductivity Eq. (1).

AC conductivity in the bond-diluted SSH chain.— To gain intuition about the role of zero modes in the low-frequency transport of disordered topological insulators, we first consider an example where bonds are removed randomly from an SSH chain [6]

$$\hat{H}_{\rm SSH} = \sum_i t_i' |i, {\rm B}\rangle \langle i, {\rm A}| + t_i |i+1, {\rm B}\rangle \langle i, {\rm A}| + {\rm h.c.}, \quad (3)$$

where t_i and t_i' take either their unperturbed values t and t' with probability $1-p$ or 0 with probability p. Since our goal is accessing the low-frequency transport at zero energy, we are interested in the structure of states around $E=0$. We assume $t' < t$.

When $p > 0$, the chain breaks down into isolated segments among which only the ones terminating with t' on both sides contribute to the low-frequency ac conductivity: these regions host pairs of zero modes in between which optical transitions are allowed in the sub-gap regime $\omega \ll |t - t'|$. To see this, consider a topological segment of length d. If d is large enough, the zero modes at its ends hybridize with each other without mixing with other states due to the finite energy gap. From perturbation theory (see [25]), the energy associated with this hybridization is proportional to the exponentially small overlap between the zero modes, $\omega = \Omega e^{-d/\xi}$, with ξ encoding the typical size of the zero mode which is proportional to its localization length $\xi_0 = \log^{-1} |t/t'|$, see [29]. It follows that the long topological segment hosts low-lying in energy resonant bonding and anti-bonding states $|\psi_\pm\rangle = (|\psi_{\rm L}\rangle \pm |\psi_{\rm R}\rangle)/\sqrt{2}$ of the zero modes at the left $|\psi_{\rm L}\rangle$ and right $|\psi_{\rm R}\rangle$ ends of the section. The dipole matrix element between the resonances takes the form

$$|\langle \psi_+|\hat{x}|\psi_-\rangle| \sim |\langle \psi_{\rm L}|\hat{x}|\psi_{\rm L}\rangle - \langle \psi_{\rm R}|\hat{x}|\psi_{\rm R}\rangle| \sim d \sim \xi_0 \log \omega, \quad (4)$$

while the density of such states per unit length arises from all topological sections of arbitrary length d, appearing with probability $(1-p)^d$. That is,

$$\nu_{\rm topo}(E) \sim \sum_d (1-p)^d \delta\left(E - \Omega e^{-d/\xi}\right) \sim |E|^{-1+2\delta}, \quad (5)$$

where in this model $\delta = (\xi/2)|\log(1-p)|$. Similar algebraic behavior of the density of states is well-known in the theory of disordered magnets [30], and a direct mapping to $1D$ random-bond Ising model can be formally established: see supplementary information (SI) in Ref. [25]. Continuing this analogy, the model given by Eq. (3) with $0 < \delta < 1/2$ is in the so-called Griffiths phase with the hybridized pairs of zero modes playing the role of the pairs of domain walls which form the rare magnetized regions [30–32].

Using Eqs. (4) and (5), we estimate the ac conductivity at low frequencies at half filling through the Kubo-Greenwood formula [20]

$$\sigma(\omega) = \frac{\pi e^2 \omega}{\hbar} \sum_{E_n \leq E_{\rm F} \leq E_m} |\langle n|\hat{x}|m\rangle|^2 \delta(E_m - E_n - \omega). \quad (6)$$

For $\omega \ll |t - t'|$, Eq. (6) reduces to the sum over all transitions between the $\psi_\pm$ pairs of resonances created by hybridizing zero modes

$$\sigma(\omega) \sim \omega \int_0^\omega dE\, \nu(E)|\langle \psi_E|\hat{x}|\psi_{-E}\rangle|^2 \delta(2E - \omega) \\ \sim \omega^{2\delta} \log^2 \omega, \quad (7)$$
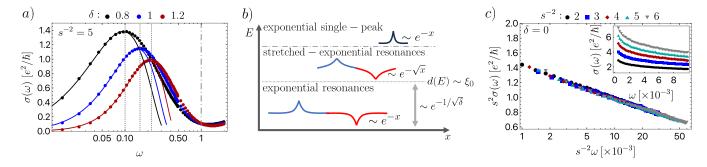
as stated in Eq. (2).

Figure 2. a) Dynamical conductivity in the SSH chain with chiral box disorder at half filling for different values of the parameter δ, which encodes the distance to the topological phase transition. The numerical data is fitted to $\sigma(\omega) = c_1 \omega^{2\delta_{\text{fit}}} \log^2(c_2/\omega)$, and $\delta_{\text{fit}} = 0.78, 1.01, 1.23$ indicate a good agreement with the actual values of δ, confirming our expression for ac conductivity in this regime (2). The crossover to the critical $\sigma(\omega) \sim \log \omega$ regime occurs beyond a certain δ-dependent frequency indicated by the dotted lines. b) Schematic representation of the crossover between different types of states found in the SSH model with bond disorder. When $\delta \neq 0$, the closest to $E = 0$ states are the hybridized exponential modes. Immediately above it lie the stretched-exponential double-peak wavefunctions arising from the surviving critical regions. At even higher energies, regular exponentially localized states are found. c) Same as a) for the critical value $\delta = 0$ and different disorder strengths s. The curves show good data collapse after re-scaling by s^2 both the frequency and the conductivity. The unscaled curves are shown in the inset. Importantly, the $\log \omega$ law holds at all disorder strengths, consistent with (10). The simulations were performed for chains of 10^3 sites and 10^6 disorder configurations.

AC conductivity away from criticality.— We now argue that conductivity retains the form of Eq. (2) for a continuous distribution of disordered bonds. To this end, consider the model defined in Eq. (3) with $t_i = t - \epsilon_i$, $t_i' = t' - \epsilon_i'$, where ϵ_i, ϵ_i' are drawn from any smooth distribution. For the numerical simulations, we assume it to be uniform within the interval $[-W/2, W/2]$.

We use real space renormalization group (RSRG) [16, 17], to obtain the properties of low-energy states in this case [25]. This method consists of identifying the largest hopping parameters and removing them from the chain using second-order perturbation theory, thus lowering the energy cutoff Ω, down from its initial value of $\Omega_0 = \max[t_i, t_i']$ (without loss of generality we fix $\prod_i t_i' < \prod_i t_i$). As this procedure is continuously repeated, the remaining effective hoppings t_{eff}' become broadly distributed $P(t_{\text{eff}}') \sim \exp\left[-2\delta \frac{\log(\Omega/t_{\text{eff}}')}{(\Omega_0/\Omega)^{2\delta}}\right]$, where the staggering parameter δ is related to the localization length at zero energy ξ_0 as $\delta = \xi_0^{-1} s^{-2}$ with

$$s^2 = a(\langle\!\langle \kappa^2 \rangle\!\rangle - \langle\!\langle \kappa \rangle\!\rangle^2), \quad \xi_0^{-1} = \langle\!\langle \kappa \rangle\!\rangle, \quad \kappa \equiv a^{-1} \log \left| \frac{t - \varepsilon}{t' - \varepsilon'} \right|. \quad (8)$$

Here, $\langle\!\langle \cdot \rangle\!\rangle$ denotes the disorder average, and a is the lattice constant.

The broad character of the distribution $P(t_{\text{eff}}')$ allows us to apply the Mott hybridization argument to the pairs of states connected by the effective t_{eff}' hoppings (cf. Fig. 1), since the bonds t_{eff}' *close in real space* are statistically likely to host pairs of zero modes that are very *far apart in energy*. Recalling that the zero modes are exponentially localized and repeating the arguments leading to Eq. (4), we conclude that Eq. (4) is also valid for the continuous distribution of bonds. A more rigorous way to

obtain Eq. (4) using the distribution $P(t_{\text{eff}}')$ is shown in [25]. Moreover, considering that the low-energy density of states retains the form of Eq. (5), $\nu(E) \sim |E|^{2\delta-1}$ [1], we conclude that Eq. (2) for the conductivity remains valid for the case of the continuous distribution of bonds. We also add that the contribution from the optical transitions which are asymmetric in energy —absent in the previously discussed case of bond-dilution [Eq. (3)]— does not affect the result as it decays faster than $\omega^{4\delta}$ at low frequencies and therefore subdominant [33].

We verify the validity of Eq. (2) by computing $\sigma(\omega)$ numerically using the Kubo-Greenwood formula Eq. (6) for the model of Eq. (3) with box disorder of ϵ_i, ϵ_i' and different values of the staggering parameter δ. As shown in Fig. 2a, Eq. (2) provides reasonable estimates for the numerical data at small frequencies.

AC conductivity at criticality.— We now consider the low-frequency behavior of the ac conductivity in the SSH chain with chiral disorder (3) at criticality, $t = t'$, with ϵ_i and ϵ_i' now drawn from the same disorder distribution, such that the condition $\prod_i t_i = \prod_i t_i'$ is satisfied. At half-filling, this model hosts a single delocalized state at $E = 0$ ($\xi_0 = \infty$) [7].

Similarly to the off-critical case in the previous section, the low-frequency ac conductivity is dominated by the transitions between isolated bonding and anti-bonding Mott resonances. In this case, all renormalized t_i, t_i' hoppings become broadly distributed with the probability $P(t_{\text{eff}}) \sim \exp\left[-\frac{\log(\Omega/t_{\text{eff}})}{\log(\Omega_0/\Omega)}\right]$ as the energy cutoff is lowered, which suppresses hybridization events between more than two zero modes, thus again justifying the application of the Mott-type pairwise hybridization argument. In the critical case, the low-energy resonances arise on either t_{eff}
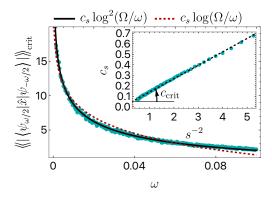
Figure 3. Dipole transition amplitude between states separated by ω with disorder strength $s^2 = 0.3$, fit to $\log^2 \omega$ (black line) and $\log \omega$ (red dashed line). The best data fit to $\log^2 \omega$ is evidence for stretched exponential behavior of the zero-energy wavefunction at criticality, justifying the result (9). Inset: coefficient c_s as a function of disorder strength s, extracted from fitting $\log^2 \omega$. The predicted relation $c_s = c_{\text{crit}} s^{-2}$ in (9) is established with $c_{\text{crit}} \simeq 0.13$. The calculation used 10^3 sites at criticality ($t = t' = 1$), with chiral box disorder, averaged over 10^4 configurations.

or t'_{eff} bonds.

The important aspect that distinguishes the critical case from the off-critical is the stretched-exponential decay of the zero mode wavefunctions at large distances $\psi_0(x) \sim e^{-s\sqrt{x}}$: this unusual spatial dependence is due to the exponent of the wavefunction undergoing a random walk, see SI [25]. Following the same argument leading to Eq. (4), we postulate the transition amplitude between the bonding and antibonding critical Mott resonances in the form

$$\langle\!\langle | \langle \psi_{\omega/2} | \hat{x} | \psi_{-\omega/2} \rangle | \rangle\!\rangle_{\text{crit}} \equiv c_{\text{crit}} s^{-2} \log^2 (\Omega/\omega) . \qquad (9)$$

This dependence is confirmed by numerical simulations, as shown in Fig. 3, with the fit to $\log^2 \omega$ agreeing exceptionally well with the data.

Combining the result of Eq. (9) and the form of the low-energy density of states, given by the Dyson singularity $\nu_{\text{crit}}(E) = s^2 [|E| \log^3 (\Omega/|E|)]^{-1}$ [1, 23], we obtain the leading low-frequency asymptote of the ac conductivity at $E_F = 0$ via the summation over transitions symmetric in energy relative to E_F, as in Eq. (7):

$$\sigma_{\text{crit}}(\omega) \sim s^{-2} \log(\Omega/\omega) . \qquad (10)$$

The scaling above is valid at any disorder strength, while the more specific form $\sigma_{\text{crit}} \sim s^{-2} \log(s^2/\omega)$ is established at low disorder (for $s \ll 1$ when $\Omega \sim s^2$ [25]). The validity of Eq. (10) and scaling with s at low disorder are confirmed numerically in Fig. 2c.

Interestingly, the logarithmic scaling (10) is also found within a certain frequency range away from criticality (cf. Fig. 2a). This behavior is due to the finite critical topological segments, which are short enough to stay unaffected by the finite localization length ξ_0, and hence remain in the form of critical stretched-exponential resonances (a detailed representation of different types of states in the SSH chain with chiral disorder is found in Fig. 2b). The crossover occurs when the frequency satisfies $\log^2 \omega \sim \xi_0$, or $\omega \sim e^{-1/\sqrt{\delta}}$. This argument clarifies the apparent mismatch between (1) and (2) at $\delta = 0$; when the staggering is decreased, the lower edge of the region hosting stretched-exponential resonances indicated with dotted lines in Fig. 2a,b approaches $E = 0$, and at any finite ω, a crossover between the two regimes occurs.

It is instructive to point out that Eq. (1) is consistent with the known result that the dc conductivity in this model grows as a square root of the size of the system $\sigma(L) \sim \sqrt{L}$ [1]. In a finite chain, the transport at the lowest possible ω occurs due to the tunneling between the two largest resonances of the size L, while, according to Eq. (9), $L \sim \log^2 \omega$.

Conclusion.— Studying the hybridization of topological zero modes in the SSH chain with chiral disorder, we demonstrated the emergence of a sub-diffusive metallic phase characterized by an activated scaling of the ac conductivity [Eq. (1)]. Remarkably, this behavior is a consequence of the type of wave function decay *only* - since the latter determines both the dipole transition amplitude between the Mott resonances and the scaling of the density of states entering the expression for the conductivity in Eq. (7). The latter statement comes from the realization that the scaling $\psi_0 \sim e^{-s\sqrt{x}}$, according to our hybridization argument, fixes the length of the typical critical state at energy ω to be $d(\omega) \sim \log^2 \omega$. This expression, in turn, dictates the typical number of modes with $|E| < \omega$, i.e., $n(\omega) \sim d(\omega)^{-1} \sim \log^{-2} \omega$, and therefore, the Dyson singularity is reproduced $\nu(E) \sim dn(E)/dE \sim |E|^{-1} \log^{-3} |E|$.

We show that the argument originally introduced by Mott to determine the ac conductivity of Anderson insulators can be extended to the critical sub-diffusive metal phase of the SSH chain, which is described by an infinite randomness fixed point. In this case, the dynamics is dominated by the pairwise hybridization of zero modes. The recognition of the crucial role played by the topological in-gap states in this transition opens a new perspective on the microscopic nature of disorder-induced topological phase transitions, such as the quantum Hall plateau transition or critical delocalization in disordered Chern insulators. Since the appearance of localized in-gap states around strong impurities is a ubiquitous feature of topological phases in any dimension [34], we anticipate that their resonant hopping will also play a crucial role in determining the existence and dynamics of topological critical points in higher spatial dimensions, which we plan to explore in future work.

----

* i.komissarov@columbia.edu
† tobiasholder@tauex.tau.ac.il
‡ raquel.queiroz@columbia.edu

[1] F. Evers and A. D. Mirlin, Anderson transitions, Reviews of Modern Physics **80**, 1355 (2008).

[2] B. Huckestein, Scaling theory of the integer quantum hall effect, Rev. Mod. Phys. **67**, 357 (1995).

[3] B. KRAMER, T. OHTSUKI, and S. KETTEMANN, Random network models and quantum phase transitions in two dimensions, Physics Reports **417**, 211–342 (2005).

[4] A. M. M. Pruisken, On localization in the theory of the quantized hall effect: A two-dimensional realization of the θ-vacuum, Nuclear Physics B **235**, 277 (1984).

[5] S. Das Sarma, Localization, metal-insulator transitions, and quantum hall effect (2007) pp. 1–36.

[6] W. P. Su, J. R. Schrieffer, and A. J. Heeger, Solitons in polyacetylene, Phys. Rev. Lett. **42**, 1698 (1979).

[7] G. Theodorou and M. H. Cohen, Extended states in a one-demensional system with off-diagonal disorder, Physical Review B **13**, 4597 (1976).

[8] A. Altland, D. Bagrets, and A. Kamenev, Topology versus Anderson localization: Nonperturbative solutions in one dimension, Physical Review B **91**, 085429 (2015).

[9] S. N. Evangelou, Spectral singularities and localisation in one- and quasi-one-dimensional systems with off-diagonal disorder, Journal of Physics C: Solid State Physics **19**, 4291 (1986).

[10] M. Inui, S. A. Trugman, and E. Abrahams, Unusual properties of midband states in systems with off-diagonal disorder, Phys. Rev. B **49**, 3190 (1994).

[11] C. M. Soukoulis and E. N. Economou, Off-diagonal disorder in one-dimensional systems, Physical Review B **24**, 5698 (1981).

[12] H. Zhang and A. Kamenev, Anatomy of topological Anderson transitions, Physical Review B **108**, 224201 (2023), arXiv:2301.04565 [cond-mat].

[13] L. Balents and M. P. A. Fisher, Delocalization transition via supersymmetry in one dimension, Physical Review B **56**, 12970 (1997).

[14] A. Gogolin, Electron localization in quasi-one-dimensional organic conductors, Physics Reports **166**, 269 (1988).

[15] E. J. Meier, A. F. An, A. Dauphin, M. Maffei, P. Massignan, T. L. Hughes, and B. Gadway, Observation of the topological anderson insulator in disordered atomic wires, Science **362**, 929 (2018), epub 2018 Oct 11, 30309909.

[16] D. S. Fisher, Random transverse field ising spin chains, Phys. Rev. Lett. **69**, 534 (1992).

[17] D. S. Fisher, Critical behavior of random transverse-field ising spin chains, Phys. Rev. B **51**, 6411 (1995).

[18] J. Bouchaud, A. Comtet, A. Georges, and P. Le Doussal, Classical diffusion of a particle in a one-dimensional random force field, Annals of Physics **201**, 285 (1990).

[19] D. Bagrets, A. Altland, and A. Kamenev, Sinai Diffusion at Quasi-1D Topological Phase Transitions, Physical Review Letters **117**, 196801 (2016), arXiv:1605.01657 [cond-mat].

[20] N. F. Mott and E. A. Davis, Electronic processes in non-crystalline materials, 2nd ed., International series of monographs on physics (Clarendon Press, Oxford, 2012).

[21] A. Abrikosov and I. Ryzhkin, Conductivity of quasi-one-dimensional metal systems, Advances in Physics **27**, 147 (1978).

[22] V. L. Berezinskiǐ, Kinetics of a quantum particle in a one-dimensional random potential, in World Scientific Series in 20th Century Physics, Vol. 11 (WORLD SCIENTIFIC, 1996) pp. 87–94.

[23] T. P. Eggarter and R. Riedinger, Singular behavior of tight-binding chains with off-diagonal disorder, Phys. Rev. B **18**, 569 (1978).

[24] R. Resta, Drude weight and superconducting weight, Journal of Physics: Condensed Matter **30**, 414001 (2018).

[25] See supplemental material, where we explain the main ingredients of the real-space renormalization group in one dimension, and give instructions on how to apply the scaling analysis to other models.

[26] A. Del Maestro, B. Rosenow, J. A. Hoyos, and T. Vojta, Dynamical conductivity at the dirty superconductor-metal quantum phase transition, Physical Review Letters **105**, 10.1103/physrevlett.105.145702 (2010).

[27] S. Gopalakrishnan, M. Müller, V. Khemani, M. Knap, E. Demler, and D. A. Huse, Low-frequency conductivity in many-body localized systems, Physical Review B **92**, 10.1103/physrevb.92.104202 (2015).

[28] O. Motrunich, K. Damle, and D. A. Huse, Dynamics and transport in random quantum systems governed by strong-randomness fixed points, Physical Review B **63**, 10.1103/physrevb.63.134424 (2001).

[29] J. K. Asbóth, L. Oroszlány, and A. Pályi, A Short Course on Topological Insulators (Springer International Publishing, 2016).

[30] T. Vojta, Phases and phase transitions in disordered quantum systems (2013) pp. 188–247, arXiv:1301.7746 [cond-mat].

[31] B. M. McCoy and T. T. Wu, Theory of a two-dimensional ising model with random impurities. i. thermodynamics, Phys. Rev. **176**, 631 (1968).

[32] R. B. Griffiths, Nonanalytic behavior above the critical point in a random ising ferromagnet, Phys. Rev. Lett. **23**, 17 (1969).

[33] Since the matrix element of the position operator for asymmetric in energy transitions is regular in ω, we estimate from (6) that $\sigma_{\mathrm{asym}}(\omega) \lesssim \omega \int_0^\omega dE\, \nu(E)\nu(E + \hbar\omega) \sim \omega^{4\delta}$.

[34] R. Queiroz, R. Ilan, Z. Song, B. A. Bernevig, and A. Stern, Ring states in topological materials, arXiv preprint arXiv:2406.03529 (2024).

[35] H. Javan Mard, J. A. Hoyos, E. Miranda, and V. Dobrosavljević, Strong-disorder renormalization-group study of the one-dimensional tight-binding model, Physical Review B **90**, 10.1103/physrevb.90.125141 (2014).

[36] R. H. McKenzie, Exact Results for Quantum Phase Transitions in Random XY Spin Chains, Physical Review Letters **77**, 4804 (1996).

[37] D. A. Ivanov, P. M. Ostrovsky, and M. A. Skvortsov, Correlations of the local density of states in quasi-one-dimensional wires, Phys. Rev. B **79**, 205108 (2009).

[38] D. A. Ivanov, M. A. Skvortsov, P. M. Ostrovsky, and Y. V. Fominov, Hybridization of wave functions in one-dimensional localization, Physical Review B **85**, 035109 (2012).

[39] R. Gade, Anderson localization for sublattice models, Nuclear Physics B **398**, 499 (1993).

Supplementary information for
"..."

Ilia Komissarov, Tobias Holder, Raquel Queiroz

In this Supplementary Information, we first review the properties of the zero-energy solutions in the SSH chain with chiral disorder. We further address analytically the hybridization of topological zero modes in the bond-diluted SSH chain. We then review certain applications of the real-space renormalization group in the SSH chain with chiral disorder. Additionally, we elaborate on the mapping between the SSH chain model (3), and the random-bond Ising model as well as the random-mass $1D$ fermion model in a continuum. Lastly, we comment on the possibility of the observation of activated dynamical scaling of ac conductivity in other disordered systems.

Notations and conventions

The lattice constant a is set to unity, unless stated otherwise. We use E and E_F to denote the reference value of the energy and the Fermi energy correspondingly. The quantity ω bears a meaning of the energy difference, hybridization energy, or the frequency of the applied ac electric field expressed in units of energy, depending on the context. With $d(E)$ we denote the characteristic spatial extent of states at energy E. We use the notation $\langle\!\langle \ldots \rangle\!\rangle$ for the disorder average reserving $\langle \ldots \rangle$ for matrix elements of operators. For the numerical simulations performed for the SSH chain with chiral disorder, we fix the sum of the inequivalent hoppings to a constant value $t + t' = 2$: the remaining free parameters of the model are therefore the difference $t - t'$ and the disorder strength W. The edge states are removed from the spectrum if present.

Wavefunctional decay of zero modes in the SSH chain with chiral disorder

In this section, we review the properties of the zero-energy states in the SSH chain with chiral disorder showing that they decay exponentially at long distances when the system is away from criticality, and stretched-exponentially (as $\psi \sim e^{-s\sqrt{x}}$) at the critical point.

We consider the Schrodinger equation $\hat{H}_\mathrm{SSH} |\psi\rangle = 0$ with the Hamiltonian

$$\hat{H}_\mathrm{SSH} = \sum_i t'_i |i, \mathrm{B}\rangle \langle i, \mathrm{A}| + t_i |i+1, \mathrm{B}\rangle \langle i, \mathrm{A}| + \mathrm{h.c.}. \tag{S11}$$

Using the real-space representation $|\psi\rangle = \sum_i (\psi_{i\mathrm{A}} |i, \mathrm{A}\rangle + \psi_{i\mathrm{B}} |i, \mathrm{B}\rangle)$, we obtain

$$t'_i \psi_{i\mathrm{A}} + t_i \psi_{i-1\mathrm{A}} = 0,$$
$$t'_i \psi_{i\mathrm{B}} + t_i \psi_{i+1\mathrm{B}} = 0. \tag{S12}$$

By iterating the above expressions, the growth(decay) rates of the zero modes localized on A and B sub-lattices are found

$$\xi_{0\mathrm{B}}^{-1} = -\xi_{0\mathrm{A}}^{-1} = \frac{1}{N} \log |\psi_{N\mathrm{A}}/\psi_{1\mathrm{A}}| = \frac{1}{N} \sum_i^N \log |t'_i/t_i| . \tag{S13}$$

Since the sum of the random quantities on the right-hand side is self-averaging, we can introduce the typical localization length of the mode localized on the B sub-lattice as defined by the law of large numbers

$$\xi_0^{-1} = \langle\!\langle \log |t'_i/t_i| \rangle\!\rangle . \tag{S14}$$

If the expression on the right-hand side is finite, the zero mode decays exponentially on average. If, on the other hand, the right-hand side vanishes, the exponent of the wavefunction, as we can see from (S13), undergoes a random walk with zero mean. The spatial decay is stretched-exponential, and characterized by a new length scale s defined in (8):

$$\langle\!\langle |\log \psi_N|^2 \rangle\!\rangle - \langle\!\langle |\log \psi_N| \rangle\!\rangle^2 = \sqrt{\left\langle\!\!\left\langle \left(\sum_{i=1}^N \log |t'_i/t_i| \right)^2 \right\rangle\!\!\right\rangle} = s\sqrt{N}, \qquad s = \langle\!\langle \log^2 |t'_i/t_i| \rangle\!\rangle - \langle\!\langle \log |t'_i/t_i| \rangle\!\rangle^2 . \tag{S15}$$

Therefore, we recover the average stretched-exponential zero mode behavior $\psi(x) \sim e^{-s\sqrt{x}}$. The qualifier *average* is extremely important here, as the critical wavefunctions would typically exhibit multiple minima and maxima due to the fluctuations in the winding number. As we are interested mainly in disorder-averaged low-frequency transport properties, the leading stretched-exponential part of the wavefunction profile suffices.
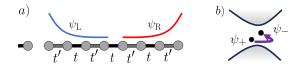
Figure S4. *a*) Two zero modes (ψ_L and ψ_R) appear on both sides of the topological region created by the bond-dilution disorder in the SSH chain. *b*) If the segment is sufficiently long, the zero modes hybridize into sub-gap bonding and anti-bonding states $\psi_\pm$. Due to the finite gap, only the optical transitions between such states (indicated with a purple arrow) will contribute to the low-frequency ac conductivity.

Mott resonances in the bond-diluted SSH chain

In this section, we obtain analytically the hybridization energy of the zero modes in the bond-diluted SSH chain model. We, therefore, consider (S11), with the hoppings missing with a probability p from the unperturbed chain with parameters t, t'.

As argued in the main text, at low frequency, only the transitions between the hybridized topological zero modes shown in Fig. S4 are relevant for transport. We therefore consider a topological segment of the length d, as shown in the image, assuming $|t'| < |t|$. The normalized unperturbed zero modes localized on the ends of the chain take the form

$$|\psi_\mathrm{L}\rangle = \sqrt{\frac{2}{\xi_0}} \sum_{0 \leq i \leq d} e^{-i/\xi_0} |i, \mathrm{A}\rangle \,,$$
$$|\psi_\mathrm{R}\rangle = \sqrt{\frac{2}{\xi_0}} \sum_{0 \leq i \leq d} e^{(i-d)/\xi_0} |i, \mathrm{B}\rangle \,,$$
$$\tag{S16}$$

where $\xi_0 = \log^{-1} |t/t'|$, and d, ξ_0 assumed large. By repeatedly using the decimation procedure outlined in the next Appendix, the Hamiltonian of the segment is reduced to

$$\hat{H}_0 = t'(t'/t)^d \hat{c}_{0\mathrm{A}}^\dagger \hat{c}_{d\mathrm{B}} + \mathrm{h.c.} \,. \tag{S17}$$

Note that the parameter is $(t'/t)^d$ is always small for sufficiently long sections, which justifies the application of the perturbation theory to obtain the low-lying in energy states. Using degenerate perturbation theory, the energies of the hybridized states $|\psi_\pm\rangle$ are found as

$$E_\pm \simeq \pm \langle \psi_\mathrm{L} | \hat{H}_0 | \psi_\mathrm{R} \rangle = \pm 2t'/\xi_0 (t'/t)^d = \pm 2t'/\xi_0 e^{-d/\xi_0} \,. \tag{S18}$$

Therefore, in the bond-diluted SSH chain, the energy of the low-lying Mott resonances depends exponentially on their size d.

Real-space renormalization group

In this section, we review the real-space renormalization group (RSRG) treatment of the SSH chain with chiral disorder (S11). The RSRG procedure consists of identifying the largest of the hoppings within the chain (suppose t_2) and decimating it using the second-order perturbation theory [35]. Consider, e.g., the $t_1 - t_2 - t_3$ cluster of hoppings described by the Hamiltonian

$$\hat{H} = \hat{H}_0 + \hat{H}_\mathrm{pert} \,, \qquad \hat{H}_0 = t_2 \hat{c}_2^\dagger \hat{c}_3 + \mathrm{h.c.} \,, \qquad \hat{H}_\mathrm{pert,} = t_1 \hat{c}_1^\dagger \hat{c}_2 + t_3 \hat{c}_3^\dagger \hat{c}_4 + \mathrm{h.c.} \,. \tag{S19}$$

The unperturbed eigenvalues are $E_0 = \pm t_2$ and the eigenstates read

$$|\psi_\pm\rangle = \frac{1}{\sqrt{2}} (\hat{c}_2^\dagger \pm \hat{c}_3^\dagger) |0\rangle \equiv \frac{1}{\sqrt{2}} (|2\rangle \pm |3\rangle) \,. \tag{S20}$$

Within the second-order perturbation theory, the effective hopping that replaces the given string $t_1 - t_2 - t_3$ is obtained as

$$t_\mathrm{eff} = \frac{\langle 1|\hat{H}_\mathrm{pert}|\psi_+\rangle \langle \psi_+|\hat{H}_\mathrm{pert}|4\rangle}{t_2} - \frac{\langle 1|\hat{H}_\mathrm{pert}|\psi_-\rangle \langle \psi_-|\hat{H}_\mathrm{pert}|4\rangle}{t_2} = \frac{t_1 t_3}{t_2} \,, \tag{S21}$$

since

$$\langle 1|\hat{H}_{\text{pert}}|\psi_+\rangle = \frac{t_1}{\sqrt{2}}, \qquad \langle 1|\hat{H}_{\text{pert}}|\psi_-\rangle = \frac{t_1}{\sqrt{2}},$$
$$\langle 4|\hat{H}_{\text{pert}}|\psi_+\rangle = \frac{t_3}{\sqrt{2}}, \qquad \langle 4|\hat{H}_{\text{pert}}|\psi_-\rangle = -\frac{t_3}{\sqrt{2}}. \tag{S22}$$

The procedure (S21) is repeated multiple times until the maximum hopping in the chain falls below the cutoff Ω. If we collectively label all odd links t' and all even links t, their distributions $P_t \equiv P_t(t, \Omega)$ and $P_{t'} \equiv P_{t'}(t', \Omega)$ will "run" with the cutoff according to

$$-\frac{\partial P_t}{\partial \Omega} = \left[P_t^{\Omega} - P_{t'}^{\Omega}\right]P_t + P_{t'}^{\Omega}\int dt_1 dt_2\, P_t(t_1, \Omega)P_t(t_2, \Omega)\delta\left(t - t_1 t_2/\Omega\right),$$
$$-\frac{\partial P_{t'}}{\partial \Omega} = \left[P_{t'}^{\Omega} - P_t^{\Omega}\right]P_{t'} + P_t^{\Omega}\int dt_1' dt_2'\, P_{t'}(t_1', \Omega)P_{t'}(t_2', \Omega)\delta\left(t' - t_1' t_2'/\Omega\right), \tag{S23}$$

where $P_t^{\Omega} \equiv P_t(\Omega, \Omega)$, and $P_{t'}^{\Omega} \equiv P_{t'}(\Omega, \Omega)$. This system of integro-differential equations was first solved by Fisher in both critical and off-critical cases [16, 17]. We review these solutions and their implications below.

Off-critical case:

For convenience, we introduce logarithmic variables

$$\Gamma \equiv \log(\Omega_0/\Omega), \qquad T \equiv \log(\Omega/t), \qquad T' \equiv \log(\Omega/t'). \tag{S24}$$

If the hoppings t are on average larger than t', the fixed point is characterized by distributions

$$P_t(T) = 2\delta \exp[-2\delta T], \qquad P_{t'}(T') = 2\delta e^{-2\delta\Gamma}\exp\left[-2\delta e^{-2\delta\Gamma}T'\right], \tag{S25}$$

i.e., the distribution for T (and therefore t) becomes cutoff-independent, while the distribution of T' becomes extremely broad already on a logarithmic scale. It implies that extremely small and isolated in energy hoppings t' appear giving rise to low-energy Mott-like resonances formed by the zero modes hybiridizing through small t' bonds. The quantity δ in the expressions above is introduced as

$$\delta \equiv \frac{\langle\!\langle T \rangle\!\rangle - \langle\!\langle T' \rangle\!\rangle}{\text{var}\, T + \text{var}\, T'}. \tag{S26}$$

The number of surviving unit cells at the scale Γ is described by the differential equation

$$dN = -N\left(P_t + P_t'\right), \tag{S27}$$

as the act of decimation always removes one unit cell. Integration of this equation yields $N \sim \Omega^{-2\delta}$. The low-energy density of states at energy E is found as $\nu(E) \sim dN^{-1}(E)/dE \sim E^{2\delta-1}$. Since almost all decimated hoppings are t-hoppings, on the approach to the fixed point, the t' hoppings become typically very long, and their lengths are therefore approximately equal to the typical length of the unit cell, i.e., $d_{t'} \sim N^{-1} \sim \Omega^{2\delta}$. The typical t' hopping itself can be found using the second distribution in (S25), as

$$t'_{\text{typ}} \sim \exp(\langle T' \rangle_{\text{D}}) \sim \exp(-\Omega^{2\delta}) \sim e^{-d_{t'}}. \tag{S28}$$

Therefore, the hybridization energy of the zero modes across such a hopping element is exponentially small in its length.

Critical case:

The distributions of T and T'

$$P_t(T) = \frac{1}{\Gamma}e^{-T/\Gamma}, \qquad P_{t'}(T') = \frac{1}{\Gamma}e^{-T'/\Gamma} \tag{S29}$$

both become extremely broad at low cutoff. The low-energy Mott resonances in this case arise on both t and t' hoppings. Solving (S27) in this case, yields the scaling of the remaining number of unit cells $N \sim \log^{-2}\Omega$, and therefore,

$d_{t'} \sim d_t \sim \log^2 \Omega$ due to the $t \leftrightarrow t'$ duality manifest in (S29). The low-energy density of states is described by Dyson singularity $\nu(E) \sim dN(E)/dE \sim (E \log^3 E)^{-1}$. Lastly, using (S29), we establishes that the remaining at low Ω hoppings are typically stretched-exponentially dependent on their lengths

$$t'_{\text{typ}} \sim t_{\text{typ}} \sim \exp(\langle T \rangle_{\text{D}}) \sim e^{-\Gamma} \sim e^{-\sqrt{d}}. \tag{S30}$$

We note here that is useful to define the dynamical critical exponent z as the polynomial part of the scaling of the typical length of the excitation with the time over which it occurs: $d^z \sim (1/\omega)$. From the discussion above, we obtain $z = 1/(2\delta)$. The polynomial part of the scaling of the density of states at small energies then reads $\nu(E) \sim E^{-1+1/z}$. Since the low-frequency ac conductivity is given by the pair-wise summation over the symmetric in energy transitions, as shown in (7), the ac conductivity is itself proportional to the density of states, and hence, $\sigma(\omega) \sim \omega^{1/z}$, up to logarithmic corrections, in consistency with (1), where $z = \infty$, and (2).

Mapping to other models

The mapping between the $1D$ Ising models and the $1D$ tight-binding models of Fermions is well-known [36]. The details of this mapping that apply to the case of an SSH chain with chiral disorder are reviewed below. Additionally, at the critical point, the properties of these lattice models are identical to the continuous model of the Dirac fermions with random mass studied extensively earlier. This allows making a host of exact statements about the properties of the SSH chain at and around criticality.

The starting point is the XX Ising model in $1D$

$$\hat{H}_{\text{Ising}} = \sum_i J_i [\hat{\sigma}_i^x \hat{\sigma}_{i+1}^x + \hat{\sigma}_i^y \hat{\sigma}_{i+1}^y], \tag{S31}$$

where $J_{i\,\text{odd}} = (t' - \epsilon_j)/2$ with random ϵ_i and $J_{i\,\text{even}} = t/2$. Using the Jordan-Wigner transformation

$$\begin{aligned}
\hat{\sigma}_i^x \hat{\sigma}_{i+1}^x &= \left(\hat{c}_i^\dagger \hat{c}_{i+1} + \hat{c}_i^\dagger \hat{c}_{i+1}^\dagger + \text{h.c.} \right), \\
\hat{\sigma}_i^y \hat{\sigma}_{i+1}^y &= \left(\hat{c}_i^\dagger \hat{c}_{i+1} - \hat{c}_i^\dagger \hat{c}_{i+1}^\dagger + \text{h.c.} \right),
\end{aligned} \tag{S32}$$

it is straightforward to show that the Hamiltonian (S31) is equivalent to the one for the SSH chain with chiral disorder (3). The dynamical spin conductivity in the model (S31) was studied in [28], where it was shown that away from the criticality (random dimer phase)

$$\sigma(\omega) \sim s^{-2} \omega^{1/z} \log^2 \omega, \tag{S33}$$

where z is the dynamical critical exponent. At criticality, [28] find

$$\sigma_{\text{crit}}(\omega) \sim s^{-2} \log \omega. \tag{S34}$$

These expressions agree with (2), (1), once we set $z = (2\delta)^{-1}$, as shown below. It is noteworthy to point out that the states giving rise to the low-frequency spin transport in this case are the hybridized domain wall states appearing on both sides of the rare regions created by the disorder in magnetic couplings. As an example, these rare regions may arise due to the large incorporations of the even-bond-ordered phase into the predominantly odd-bond-ordered environment. Such hybridized domain walls are non-local duals of the Mott resonances described in the main text.

Some further exact analytical results for the SSH chain follow from the low-energy theory for the Hamiltonian (3) expanded around $k_{\text{F}} = \pi$

$$\hat{H}_{\text{cont}} = \sum_x \hat{c}_x^\dagger [iv_{\text{F}} \hat{\sigma}_2 \partial_x + (t' - t - \varepsilon_x) \hat{\sigma}_1] \hat{c}_x, \tag{S35}$$

where $v_{\text{F}} = t$. In the extensive studies of this model summarized in [36] it was established that away from criticality, $\nu(E) \sim E^{-1+2\delta}$ and the dynamical critical exponent $z = (2\delta)^{-1}$. At criticality ($\delta = 1$), the density of states takes the form of the Dyson singularity $\nu(E) \sim s^2 [|E| \log^3 (s^2/|E|)]^{-1}$. The results found within this continuum model apply to the full tight-binding case (3) when the dimerization is small and the disorder is low, i.e. $t \gg |t - t'|$, $s^2 \ll 1$.

General scaling considerations

The result $\sigma_{\text{crit}}(\omega) \sim \log \omega$ was obtained in the main text by applying general arguments regarding the hybridization of localized wavefunctions originally used by Mott to determine dynamical conductivity in single-band models [20] and can be generalized to materials of higher dimensionality [37, 38]. We may ask, therefore, under which conditions such a tunneling scaling of ac conductivity may hold in a generic system. To address this question, let us consider the family of impurity wavefunctions decaying as $\psi(\mathbf{r}) \sim e^{-r^{1/\alpha}}$ at large distances, with α being a free parameter to be constrained. In order to remove the coefficient ω in the expression for the conductivity (6), the density of states should assume the form $\nu(E) \sim (|E| \log^{\beta} |E|)^{-1}$. Graphene with chiral disorder, for instance, has a DOS singularity of this type [39]. Assuming chiral symmetry and performing the pairwise symmetric summation as in (7), we obtain a general scaling criterion,

$$\sigma(\omega) \sim \log^{2\alpha-\beta} \omega \,, \tag{S36}$$

i.e., the requirement $\alpha > \beta/2$ must hold in order to obtain a sub-diffusive metal with purely activated scaling at low ω. For the SSH chain, $\alpha = 2$ and $\beta = 3$, which satisfies this criterion. It will be interesting to investigate the phenomenology imposed by (S36) in other disordered, topological systems, which is a subject of future work.